

1 TITLE PAGE

2 **Drones as tools for coastal monitoring: multi-temporal analysis of beach**
3 **topography.**

4
5 **Elisa Casella**^{1,2}, **Alessio Rovere**^{3,4}, **Andrea Pedroncini**⁵, **Colin P. Stark**⁴, **Marco**
6 **Casella**⁶, **Marco Ferrari**¹, **Marco Firpo**¹.

7 ¹ DISTAV, University of Genoa, Italy

8 ² SEAMap srl, Environmental Consulting, Italy

9 ³ MARUM & ZMT, University of Bremen, Sea Level and Coastal Change research group, Germany

10 ⁴ Lamont-Doherty Earth Observatory, Columbia University, USA

11 ⁵ DHI-Italia, Genova, Italy

12 ⁶ Freelancer and Professional UAV pilot, Italy

13
14
15
16 **Corresponding author:**

17 **Elisa Casella, PhD, University of Genoa, DISTAV, Corso Europa, 26 16132, Genova,**
18 **Italy, elisacasellaphd@gmail.com**

19
20
21
22 **Published in Geo-Marine Letters on 26 January 2016**
23 **Volume 36 (2016) 151 –163**
24 **<https://doi.org/10.1007/s00367-016-0435-9>**
25
26

27 **Abstract**

28 The application of light Remotely Piloted Aircraft Systems (RPAS, or drones) coupled with
29 Structure from Motion and Multi-View Stereo techniques in earth sciences is increasing,
30 especially for which concerns the monitoring of the rapid evolution of geomorphological
31 features. In this paper, the topographic changes of a stretch of coastline in North-Western
32 Italy have been studied. The same stretch of coastline has been surveyed three times in 5
33 months, obtaining digital elevation models and orthophotos of the beach. The difference in
34 beach topography between each time step has been calculated, and changes in beach
35 topography in light of sea storms and human activities affecting the area have been
36 investigated. The results show that drones and photogrammetry are low-cost, high-
37 resolution and efficient tools that can be employed effectively to map changes of beach
38 topography through time, which in turn are essential for beach management actions.

39
40 **Keywords** Beach erosion, Drones, RPAS, Beach monitoring, Unmanned Aerial Vehicles

41
42 **1. Introduction**

43 Coastal erosion is one of the main natural processes defining the evolution of a shoreline
44 through time. Along beaches, erosion removes sediment from the coastal system and
45 transports it offshore throughout the action of waves and currents. In general, coastal
46 erosion is considered a problem in need of management when it occurs in areas where the
47 human occupation of the coast is significant. At global scale, common figures state that the
48 global population density within 100 kilometers of the coastline is nearly 3 times higher
49 than the global average density (Small and Nicholls, 2003), and that 10% of the human
50 population is living less than 10 meters above sea level (McGranahan et al., 2007). An
51 often-cited number states that 70% of the world's soft coasts are suffering erosion

52 problems (Bird, 1987).

53 The management and decision-making process in coastal areas is often based on studies
54 investigating rates and modes of coastal changes, which can be derived from different
55 kinds of beach monitoring, either direct (i.e. GPS surveys on the shoreline or topographic
56 transects) or indirect (e.g. lidar or aerial photography). Recently, new survey techniques
57 based on Remotely Piloted Aircraft Systems (RPAS), often also called Unmanned Aerial
58 Vehicles, UAVs, or drones) started to be employed in geomorphological and ecological
59 studies (Everaerts 2008; Colomina & Molina 2014; Anderson & Gaston 2013), and are
60 becoming common survey methods. The most common geomorphological application of
61 RPAS consists in mounting a camera on a rotor-wing or fixed-wing remotely controlled or
62 programmed aircraft and taking almost-nadir pictures of the ground that are then analysed
63 with Structure from Motion (SfM) and Multi-View Stereo (MVS) reconstruction algorithms to
64 obtain Digital Elevation Models (DEMs) and orthophotos of the terrain.

65 At present, studies are starting to go beyond the simple assessment of the accuracy of
66 orthophotos and DEMs that can be obtained with RPAS and SfM with MVS techniques,
67 and to use RPAS to obtain data to address specific environmental or geological problems
68 (Niethammer et al. 2012; Casella et al., 2014; Woodget et al., 2014; Elmer et al., 2014;
69 Peréz-Alberti and Trenhaile, 2014). In this paper the data obtained with RPAS has been
70 used to assess coastal changes of a beach in Northern Italy (NW Mediterranean) over a
71 period of 5 months. Drones are closing the gaps in small scale remote sensing (Berni et
72 al., 2009; Watts et al., 2012), as they allow the acquisition of topographic data at low
73 altitude and their cost allows to repeat survey at short time spans. The coastal zone seems
74 to be an ideal ground for the application of multi-temporal RPAS surveys, as the evolution
75 of these environments happens often fast and requires efficient, low-cost and sufficiently
76 accurate monitoring techniques.

77 **2. Methods**

78 **2.1 Study area**

79 Our study area is located in Liguria, an Administrative Region of Italy in the NW
80 Mediterranean (Fig.1c). The region is often hit by severe storms (Parodi et al 2012; Rebola
81 et al 2013; Fiori et al 2014) associated with sea storms, which put in danger population
82 and cause several damages to the coastal zone (Orlandi et al. 2008; Pasi et al. 2011). Due
83 to the importance of coastal erosion problems in the Region, several research initiatives
84 have been directed towards understanding the dynamics of its coastal areas (e.g.
85 Brignone et al., 2012), and monitoring the evolution of the coastal system with different
86 techniques (e.g. Vacchi et al., 2012; Casella et al., 2014). Recently, the Liguria Regional
87 Authority has made available vector files of the shoreline (wet/dry line) extracted from
88 orthophotos made in 1944, 1973, 1983 and 2003. The first flight was done by the UK
89 Royal Air Force during WWII, while the latter were performed with the aim of documenting
90 the shoreline changes that started to affect the Region after the economic boom of the 60's
91 and 70's. In those years, both the population and the tourism industry grew exponentially
92 in the coastal parts of the Region (Fierro et al., 2010).

93 The focus of our study is a part of the shore of the municipality of Borghetto Santo Spirito,
94 a small coastal town of western Liguria. The evolution of the coastal area of this town is
95 representative of the evolution of many Northern Mediterranean coastal areas. Borghetto
96 was a small village at end of 1800, when the railroad was constructed to connect the main
97 cities of Genoa (Italy, to the East) and Nice (France, to the West). Materials for the
98 construction of the railroad were quarried from a local watercourse, named Varatella river,
99 causing the reduction of the sediment input in the budget of sediments of the beaches.
100 This led to the erosion of the coastline (Fierro et al., 2010). Since the construction of the
101 railroad, the coastline has been affected by engineering works (e.g. groynes, parallel
102 defences) that were aimed primarily at protecting the railway from sea storms. In 1944, the
103 shoreline was running near the railway (Fig.1a). From the 60s to nowadays, the shoreline

104 has been object of several interventions of beach nourishment and coastal engineering
105 that allowed the creation of beaches, which started to be exploited for tourism purposes
106 (Fig. 1a, Ferro et al., 2010). The most recent engineering work (2006-2008) are three
107 artificial islands located in the western part of the town (Fig. 1b), that have been associated
108 to two major beach nourishments in 2003 and 2007 (Fig. 1a), with a total amount of 13,900
109 m³ of sediment discharged in the area. This part of the town is the most affected by coastal
110 erosion problems, as all sediment inputs are blocked by a rocky promontory (Capo Santo
111 Spirito) to the west and by a major groyne that blocks the input of sediments from the
112 Varatella River to the east.

113 As it was the subject of repeated beach interventions to mitigate coastal erosion, the
114 westernmost part of the town (Fig. 1b) was the object of several beach monitoring
115 campaigns, which consisted mostly in differential GPS (DGPS) surveys of the wet-dry line
116 (Fig. 1b) and bathymetric surveys. The results of those surveys indicate that, following the
117 interventions in this area, the shoreline has advanced and now it fluctuates yearly around
118 a new equilibrium. In winter 2013-2014, a portion of this area using a camera mounted on
119 a RPAS platform has been surveyed, with the aim of documenting the evolution of the
120 beach topography of this beach at sub-yearly scale and relating coastal changes to sea
121 storms hitting the shoreline in the periods between the surveys.

122 *2.2 Remotely Piloted Aircraft Systems (RPAS), photogrammetry and GIS tools.*

123 In this work a RPAS (Mikrokoetter Okto XL) equipped with a Canon G11 camera has been
124 used to obtain aerial pictures with 3648x2736px resolution. The maximum take off weight
125 of the RPAS was of 1.8 Kg. Flights were programmed using the Mikrokoetter OSD tools
126 software to cover the entire area shown in Fig. 1b. The altitude of the flight was 70m, the
127 speed 1 m/s and the shoot was one picture every 2 seconds. During our flights, one pilot
128 and one observer have been employed. The pilot had the duty to perform take-off and
129 landing operations and interrupt the GPS-guided flight in case of unexpected behaviour of

130 the RPAS. The observer had the duty to follow the flight on the ground station and
131 communicate to the pilot changes from the predefined path. There are laws for flying
132 RPAS that vary according to countries and operative scenarios. An overview of national
133 regulations is contained in Colomina and Molina, 2014. For a more detailed description of
134 the system used in this paper, see Casella et al., 2014.

135 In order to generate DEMs and orthorectified images from near-nadir photos acquired
136 during our flights Agisoft Photoscan (<http://www.agisoft.ru>) has been used. Photoscan is a
137 software that orients and matches automatically large datasets of images, and processes
138 them in four main steps. As a first step, the software aligns the photographs using a SfM
139 algorithm (Ullman, 1979). The SfM algorithms detect image feature points and
140 subsequently monitor the movement of those points throughout the image dataset. This
141 information is used as input to estimate the locations of those feature points and to render
142 them as a sparse three-dimensional point cloud.

143 Estimation of the camera position is one of the main components in SfM, since SfM
144 algorithms mainly depend on the accurate knowledge of the camera positions (Hartley and
145 Zisserman 2003; Szeliski 2010). Outputs of this first step are: (i) a point cloud of three-
146 dimensional points representing the geometry of the study area; (ii) the camera positions
147 at the moment of image acquisition; (iii) the internal calibration parameters (focal length,
148 principal point location, three radial and two tangential distortion coefficients). Since these
149 first processing steps estimate the calibration parameters, there is no real need to apply
150 calibrated cameras and optics during the image acquisition stage (Verhoeven, 2011). The
151 second step builds a dense point cloud. In coastal zone surveys, most pictures are
152 partially occupied by the sea, which must be excluded from the beach topography. To
153 remove the sea from the calculation of the point cloud, the Photoscan mask function which
154 allows to remove manually selected area has been used. In the third step, the algorithms
155 operate on the pixel values to build the majority of geometric details. All pixels are utilized

156 in the MVS reconstruction algorithm (Scharstein and Szeliski, 2002; Seitz et al., 2006),
 157 which enables proper handling of fine details present in the scenes and represents them
 158 as a mesh. In this step, the software applies an algorithm based on an advanced computer
 159 vision solution that enables the creation of high-quality three-dimensional content from a
 160 series of overlapping aerial images (Verhoeven, 2011). In the fourth step, the mesh is
 161 textured with the photographs. From Agisoft Photoscan, the orthophoto and the DEM have
 162 been exported into a GIS software. With this, after the georeferencing procedure described
 163 below, differences between the co-registered DEMs have been calculated.

164 In order to georeference the DEM and orthophotos produced with Agisoft Photoscan, 8
 165 Ground Control Points (GCPs) collected using a GPS system (Trimble ProXRT) have been
 166 used. 10 minutes of static data at each point has been collected, and postprocessed using
 167 the 1-second data of the GNSS base station 'Istituto G. Falcone'
 168 (<http://www.gnssiguria.it/postprocessing.html>), which is located 1.5 Km from our study
 169 area. The final accuracy of our GPS data is better than ± 10 cm (XYZ). All our elevations
 170 were referred to the EGM 2008 global geoid model. As targets for the GCPs, fixed
 171 structures on the ground, such as the centre of sewer covers, mosaics on the ground such
 172 as edges of structures or the centre of boulders forming the groynes have been used.

173 Permanent structures can be recognized in different set of photos taken at different times,
 174 allowing to georeference each set using the same GCPs, reducing the survey time. An
 175 alternative method is to place mobile targets for the time of the flight, such as rectangular
 176 coloured sheets and repeat the GPS survey every flight.

177 During the GPS survey additional control points (CPs) along continuous GPS transects on
 178 invariant surfaces (e.g. concrete structures or walking areas not subject to change in time)
 179 have also been collected. The GPS data has been postprocessed using the 1-second data
 180 of the GNSS base station 'Istituto G. Falcone' and points having vertical accuracy higher
 181 than 10 cm (e.g. 15 cm) have been discarded. For each dataset, the Root Mean Square

182 Error (RMSE) between the CPs and the values of the DEM at the same location has been
 183 calculated. The RMSE was calculated using the equation:

$$184 \quad RMSE = \sqrt{\frac{\sum_{i=1}^n (CP_i - D_i)^2}{n}} \quad (1)$$

185 where CP is the elevation of the CP measured with post-processed GPS data, D is the
 186 elevation of the DEM at the same point and n the total number of CPs.

187 In order to compare the DEM with the shoreline surveyed with DGPS, the wet/dry line has
 188 been traced on the orthophotos. The wet/dry line is the boundary between wet and dry
 189 sand. Thanks to the calm sea conditions during our flights, the low tidal ranges and the
 190 high inclination of the beach profile, this coincides roughly with mean sea level at the time
 191 of measuring.

192 3. Results

193 3.1 RPAS Flights, accuracy of DEMs and sea conditions between the surveys

194 In this study, three flights have been done, covering the same area (~ 0.01 km²) at different
 195 times. Each flight resulted in a total of ~ 130 photos shot at $\sim 90^\circ$ angle. Excluding blurred
 196 or moved pictures and the areas where less than 9 pictures overlapped, 65-70 pictures for
 197 each flight have been used as input for the software workflow. The time to collect a single
 198 set of pictures was 8 minutes (using one battery for each flight). The survey has been
 199 repeated the 1 November 2013, 4 December 2013, 17 March 2014 using the same flight
 200 parameters. After comparing the elevation of CPs and DEMs at 254 points, the vertical
 201 accuracy of the DEMs has been determined as 0.15-0.16 m (RMSE, Fig.2).

202 As regards accuracy of the DEM, a further analysis involving the number of pictures
 203 overlapping at each survey has been done. Fig.2 shows that there are areas where less
 204 than 4 pictures overlap. In these areas (gray in Fig.2) the DEM has been extracted

205 anyway, but it has been considered not reliable in our multitemporal analysis.

206 In order to understand the natural drivers of coastal changes in the study area Fig.3 shows

207 an analysis of wave data in the period between our three surveys. First, wave data

208 (significant wave height, mean wave direction and peak period) from the Capo Mele buoy,

209 which is part of the Liguria Region buoy network (<http://servizi-meteorologia.arpa.gov.it/boacapoemele.html>) has been downloaded. The buoy is located about 20 km south of the

210 study area (43°55'18"N 8°10'50"E). From this dataset, all the sea storms that had a

211 significant wave height of more than 2 meters at the buoy (gray lines in Fig.3) have been

212 extracted and used as input to MIKE 21 Spectral Wave (SW) model developed by DHI

213 (former Danish Hydraulic Institute). MIKE 21 SW model has been implemented for the

214 study area using the mesh grid and the configuration described in Casella et al., 2014. The

215 model has run for each sea storms and wave data have been extracted from the output of

216 each run at about 500 m offshore of the study area (black lines in Fig.3).

217 In the period between the first two surveys (1 November–4 December) the wave buoy

218 registered two sea storms (Fig.3, upper part), which hit the study area mainly at a E-NNE

219 angle and low intensities (significant wave height less than 0.5 meters the first sea storm,

220 around 1-1.5 meters the second). In the period between the second and the third survey (4

221 December-17 march 2014) the study area was hit by four sea storms with prevailing SE

222 direction (Fig.3, lower part), all of them reaching peak wave heights of 1.5-2 meters.

223

224 **3.2 Coastal changes**

225 Fig.4 shows the results of the difference between DEMs obtained for our study area at

226 different times. In the left frame, the difference between the DEM obtained the 1st of

227 November and the 4th of December 2013 shows four patterns of change. In the

228 southernmost tip of our study area, volume changes indicate that sediment has been

229 quarried from the beach and brought landward. Calculating the volume of the accumulated

230 material it has been calculated that ~518.9 m³ of material have been moved using an

231 automatic excavator. The track marks of the excavator are evident in the orthophoto taken

232 the 4th of December 2013. Another volume change is a net erosion in the central part of

233 the beach (marked with number 1 in Fig.4). Here, around 632 m³ are missing in the DEM

234 of the 4th of December. Analysis of the orthophotos shows that the missing material is a

235 grove of reeds that was cut between the 1st of November and the 4th of December. Retreat

236 of the wet-dry line, lowering of the beach profile in the northernmost part and aggradation

237 of the beach in the central part provide evidence that, although small, the sea storms

238 hitting the area between our first two survey (Fig.3, upper part) caused significant beach

239 topography changes. As the eroded volume of sediment does not match the volume of the

240 aggradation, there might be a sediment input from the submerged beach and from the

241 beaches located east of our study area (see Fig.1b).

242 A very different evolution can be inferred from the comparison of the DEMs obtained

243 between the 4th of December 2013 and the 17th of March 2014 (right panel in Fig. 4). The

244 strong southeastern sea storms hitting the shoreline in this period caused the progradation

245 of the shoreline to its summer position (compare the shoreline surveyed the 17th of March

246 2014 with the June shoreline surveyed with DGPS, shown as dashed line in Fig.4) and the

247 general aggradation of the beach profile. As only a minor area of erosion can be identified

248 in the southernmost tip (where the presence of the rocky promontory of Capo Santo

249 Spirito, Fig.1b, blocks further sediment inputs), it is likely that a large part of the sediments

250 come from the shallow submerged area in front of the beach.

251 **4. Discussions**

252 **4.1 RPAS as beach monitoring technique**

253 Techniques for beach monitoring can be divided in two major categories: those based on

254 *in situ* observations and those employing analysis of remotely sensed data. Among the first

255 ones the most used are high-accuracy GPS surveys (Morton et al., 1993; Harley et al.,

256 2010) and total stations or terrestrial laser scanners (Lee et al., 2013). These techniques

257 are relatively inexpensive and have a good accuracy (2-6 cm vertical, Lee et al., 2013) but
258 they require large efforts to map wide areas. Common techniques to map larger areas in
259 shorter times are remotely sensed data, such as aerial photographs or webcam images
260 (Hapke and Richmond, 2000; Taborda and Silva, 2012), satellite images taken at different
261 times (Blodget et al., 1991) or airborne lidar mapping (Stockdon et al., 2002). Such
262 techniques have as main limitations their cost and the availability of images in periods of
263 interest.
264 Beach monitoring is subject to a trade-off between time, cost, accuracy and resolution of
265 the survey (both spatial and temporal). As an example, if one wants to understand the
266 short-time evolution (weeks to months) of a coastal system, traditional in situ
267 measurements can be used with sufficient temporal resolution (i.e. they can be used to
268 map the evolution of an area on a monthly basis), but they allow to map limited areas and
269 can provide only limited three dimensional information (e.g. along transects). On the other
270 side, airborne orthophotography and lidar provide good spatial resolution, but their cost
271 often does not allow performing surveys at short time intervals. Similar trade-offs are
272 common in other research disciplines, such as habitat monitoring or wildlife conservation,
273 where capturing short-term changes of an observed phenomenon is often limited by the
274 observation technique employed.
275 The use of small RPAS for remote sensing, landscape mapping and environmental
276 monitoring allows to partially overcome such problems since they can provide data at high
277 and customly-adjustable frequency (Everaerts, 2008; Delacourt et al., 2009; Niethammer
278 et al., 2010; Niethammer et al., 2012; Hugenholz et al., 2013; Stumpf et al., 2013;
279 Ouedraogo et al., 2014). Typically, small RPAS are relatively low cost (5-10K €), and their
280 limited dimensions (few tens of centimeters and usually < 5kg) make them easily and
281 rapidly deployable. In our study area, RPAS allowed us to obtain orthorectified
282 photographs and DEMs of the same coastal area at three times over a period of 5 months.

283 As regards the survey efficiency, the study area (0.01 km²) has been mapped with a flight
284 of 8 minutes. This translates into a survey efficiency of 7.5 Ha per hour, which is low if
285 compared with airborne surveys (e.g. lidar) but is high compared to laser scanner or DGPS
286 surveys. The final vertical accuracy (± 16 cm) of the DEM produced is in line with most
287 studies using similar techniques in similar areas (Mancini et al., 2013), but is low if
288 compared to lidar or most traditional direct survey techniques (typically 2.5-5 cm). It is
289 worth noting that the smoothness and uniformity of sediment surfaces limits the
290 effectiveness of matching algorithms (Mancini et al., 2013). Similar problems might be
291 created by water reflections, which should be masked to avoid unwanted errors in the
292 matching process.
293 *4.2 RPAS multi-temporal surveys: a support to coastal zone management*
294 The results obtained in our study also have some management implications. First, it has
295 been documented the possibility to detect changes due to human activity that involve the
296 movement of sediments on the beach and the removal of vegetation. Moving or nourishing
297 sediments on the beach is considered analogous to beach nourishment (Regional Laws
298 13/1999, 6/2001, 3/2007 and 5/2011, which receive National and EU framework
299 directives). The Regional Laws state that if more than 10m³ of sediment per linear meter
300 are moved on the shoreline, the subject in charge of the movement is required to perform
301 an environmental evaluation of the action. This evaluation should include description of the
302 site, source and quantity of sediments involved and considerations on potentially
303 threatened habitats or species. In Italy, the subject in charge of the action is not
304 necessarily a public authority, but is in many cases a private beach manager, who receives
305 the right to use the beach from the State for a number of years for commercial purposes in
306 exchange of a yearly rent.
307 Regional Authorities may choose to employ RPAS multi-temporal surveys for the control of
308 such actions. The movement of sediments usually take place in late October along the

309 Liguria coastline (as well as other Italian coastlines), therefore one flight at the end of the
310 summer season (September) and one in November should catch all the sediment
311 movements done along the coast. In fact, once DEM and orthophoto are extracted,
312 volumes of sediments moved or imported to a beach can be calculated using common GIS
313 tools. Another management implication of the multi-temporal survey presented is found in
314 the application of drones to obtain data on the short-term evolution of the beach
315 topography after the placement of an infrastructure (according to regional law 1793/2005),
316 like the ones present in the study area.

317 Analyzing changes in beach topography in light of the intensity and direction of sea storms
318 hitting the shoreline, it is possible to gather some information on the short-term dynamics
319 related to the coastal defences that have been recently placed in the study area. Looking
320 only at the yearly evolution of the shoreline (Fig.1b) it might be concluded that after the
321 emplacement of those defences the shoreline has advanced, and since then it oscillates
322 around an average position. Our data suggests that when the shoreline retreats after
323 smaller sea storms from the East (left panel of Fig.4), there is a volume gain on the
324 emerged beach and virtually no loss of sediments towards the submerged beach. When a
325 series of strong storms from Southeast hits the shoreline, our data suggest that the beach
326 responds with an aggradation and progradation of the beach topography, and possibly
327 there is a net transport of sediments from the submerged beach to the emerged one (right
328 panel in Fig.4). Also in this case, no sediment appears to be lost from the emerged beach
329 towards the submerged area. It is worth noting that three average-intensity southeastern
330 sea storms are enough to shift the shoreline to its summer position.

331 5. Conclusions

332 Beach erosion is a significant natural process, which affects coastal population and
333 properties. The management of sandy coasts relies on beach monitoring to gather data on
334 the intensity and rates of beach evolution, and monitoring is subject to trade-offs between

335 accuracy, costs and resolution of the survey.

336 The last four years have seen an exponential increase of research activities based on data
337 collected from drones. Flying platforms have become smaller and capable of lifting more
338 weight, and sensors are starting to be tailored specifically for drone applications. The
339 learning curve for drone pilots is becoming less steep, and is counterbalanced by national
340 regulations putting limits to the flying areas, and requiring among other things specific pilot
341 training and risk assessments of the flight operations. In coastal environments, the
342 application of SfM and MVS methods from drone photographs may prove challenging
343 due to the uniform nature of the landscape. Also, flights in coastal areas might be difficult
344 due to the risks of gusty winds or rapid changes in meteorological conditions, and
345 corrosion due to marine spray requires a frequent maintenance of the drone.

346 For these reasons, coastal areas are one of the most challenging environments for drone-
347 based research. On the other side, the rapid rates and the entity of changes along most
348 coastal zones, especially sandy beaches, make them the ideal ground for the application
349 of such tools. In this study it has been demonstrated that methods employing aerial
350 photographs from drones analysed with SfM and MVS algorithms can be effectively used
351 for multi-temporal monitoring of coastal areas, and the data obtained can be used for
352 management purposes. Our results are accurate enough to provide information on how
353 the study area evolved in a period of 5 months, and have been obtained with a survey
354 efficiency and cost that is unmatched by other common survey techniques.

355 Acknowledgments

356 This work is part of the project MIRAMAR, funded by the PO CRO European Social Fund,
357 Regione Liguria 2007-2013 Asse IV "Capitale Umano / Human Capital". A. Rovere
358 acknowledges for funding the Institutional Strategy of the University of Bremen, funded by
359 the German Excellence Initiative and ZMT, the Leibniz Center for Tropical Marine Ecology.
360 The authors wish to acknowledge C. Cavallo and Regione Liguria for providing baseline

361 data and local datasets. We thank Matteo Vacchi (CEREGE, CNRS) and Luigi Mucerino
 362 (University of Genoa) for useful discussions. The authors are grateful to MEDFLOOD
 363 INQUA 1203 project for discussion and input during the Athens meeting in 2013. We
 364 acknowledge Geom. A. Billeci and the staff of the Municipality of Borghetto S.S. for
 365 collaboration.

366 **References**

367 Anderson K, Gaston KJ (2013). Lightweight unmanned aerial vehicles will revolutionize
 368 spatial ecology. *Frontiers in Ecology and the Environment* 11: 138–146.
 369 <http://dx.doi.org/10.1890/120150>

370 Berni JAJ, Zarco-Tejada PJ, Suárez L, Fereres E (2009). Thermal and narrowband
 371 multispectral remote sensing for vegetation monitoring from an unmanned aerial
 372 vehicle. *IEEE Transactions on Geoscience and Remote Sensing* 47: 722-738.

373 Bird E (1987). The modern prevalence of beach erosion. *Marine Pollution Bulletin* 18: 151–
 374 157.

375 Blodgett HW, Taylor PT, Roark JH (1991). Shoreline changes along the Rosetta-Nile
 376 Promontory: monitoring with satellite observations. *Marine Geology* 99: 67–77.

377 Brignone M, Schiaffino CF, Isla FI, Ferrari M (2012). A system for beach video-monitoring:
 378 Beachkeeper plus. *Computers & Geosciences* 49: 53–61.

379 Casella E, Rovere A, Pedroncini A, Mucerino L, Casella M, Cusati LA, Vacchi M, Ferrari M
 380 Firpo M (2014). Study of wave runup using numerical models and low-altitude aerial
 381 photogrammetry: A tool for coastal management. *Estuarine, Coastal and Shelf
 382 Science*, 149: 160-167. doi:10.1016/j.ecss.2014.08.012

383 Colomina I, Molina P (2014). Unmanned aerial systems for photogrammetry and remote
 384 sensing: A review. *ISPRS Journal of Photogrammetry and Remote Sensing* 92: 79–97.

385 Delacourt C, Allemand P, Jaud M, Grandjean P, Deschamps A, Ammann J, Cuq V, Suanez
 386 S (2009). DRELIO: an unmanned helicopter for imaging coastal areas. *Journal of*

387 Coastal Research Special Issue 56: 1489–1493.

388 Eltner A, Baumgart P, Maas HG, Faust D (2014). Multi-temporal UAV data for automatic
 389 measurement of rill and interrill erosion on loess soil. *Earth Surface Processes and
 390 Landforms*. doi: 10.1002/esp.3673

391 Everaerts J (2008). The use of unmanned aerial vehicles (UAVs) for remote sensing and
 392 mapping. *The International Archives of the Photogrammetry, Remote Sensing Spatial
 393 Information Sciences XXXVII Part B1*, Beijing 2008.

394 Fierro G, Berrilo G, Ferrari M (2010). Le spiagge della Liguria occidentale – analisi
 395 evolutiva. Regione Liguria – Ass. Pianificazione territoriale, Urbanistica Ed., 174 pp.

396 Fiori E, Comellas A, Molini L, Rebora N, Siccardi F, Gochis DJ, Tanelli S, Parodi A (2014).
 397 Analysis and hindcast simulations of an extreme rainfall event in the Mediterranean
 398 area: The Genoa 2011 case. *Atmospheric Research*: 138, 13-29.

399 Hapke C, Richmond B (2000). Monitoring beach morphology changes using small-format
 400 aerial photography and digital softcopy photogrammetry. *Environmental Geosciences*:
 401 7, 32–37.

402 Harley MD, Turner IL, Short AD, Ranasinghe R (2010). Assessment and integration of
 403 conventional, RTK-GPS and image-derived beach survey methods for daily to decadal
 404 coastal monitoring. *Coastal Engineering*: 58, 194–205.

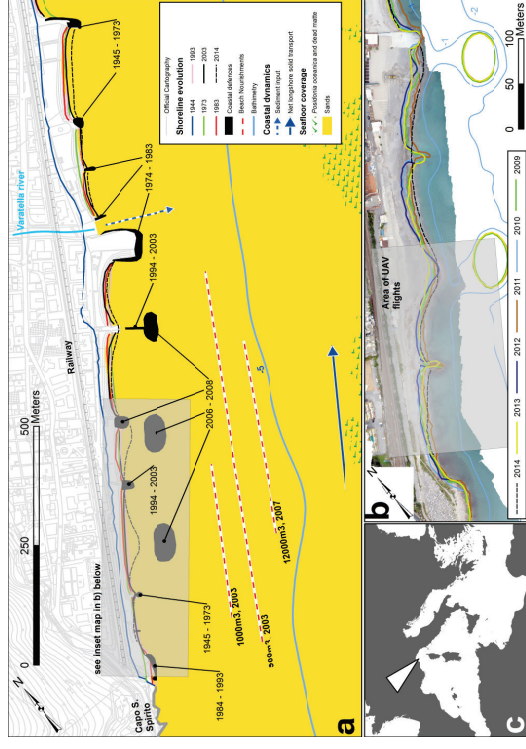
405 Hartley R, Zisserman A (2003). *Multiple View Geometry in Computer Vision*. Cambridge
 406 University Press: Cambridge.

407 Hugenholz CH, Whitehead K, Brown OW, Barchyn TE, Moorman BJ, LeClair A, Riddell K,
 408 Hamilton T (2013). Geomorphological mapping with a small unmanned aircraft system
 409 (sUAS): feature detection and accuracy assessment of a photogrammetrically-derived
 410 digital terrain model. *Geomorphology*: 194, 16–24.

411 Lee JM, Park JY, Choi JY (2013). Evaluation of Sub-aerial Topographic Surveying
 412 Techniques Using Total Station and RTK-GPS for Applications in Macrotidal Sand

- 413 Beach Environment. *Journal of Coastal Research, Coastal Education & Research*
 414 Foundation, Special Issue: 535–540.
- 415 McGranahan G, Balk D, Anderson B (2007). The rising tide: Assessing the risks of climate
 416 change and human settlements in low elevation coastal zones. *Environment and*
 417 *Urbanization*: 19, 17–37.
- 418 Morton RA, Leach MP, Paine JG, Cardoza MA (1993). Monitoring beach changes using
 419 GPS surveying techniques. *Journal of Coastal Research*: 702–720.
- 420 Niethammer U, Rothmund S, James MR, Travelletti J, Joswig M (2010). UAV-based
 421 remote sensing of landslides. *Int. Arch. Photogram. Rem. Sens. Spatial Inf. Sciences*,
 422 vol. XXXVIII. ISPRS Comm. V., Newcastle-upon-Tyne, U.K.
- 423 Niethammer U, James MR, Rothmund S, Travelletti J, Joswig M (2012). UAV-based
 424 remote sensing of the Super Sauze landslide: evaluation and results. *Engineering*
 425 *Geology*: 128, 2–11.
- 426 Ouédraogo MM, Degré A, Debouche C, Lisein J (2014). The evaluation of unmanned
 427 aerial system-based photogrammetry and terrestrial laser scanning to generate DEMs
 428 of agricultural watersheds. *Geomorphology*: 214, 339–355.
- 429 Orlandi A, Pasi F, Onorato LF, Gallino S (2008). An observational and numerical case
 430 study of a flash sea storm over the Gulf of Genoa. *Advances in Science and Research*:
 431 2, 107–112.
- 432 Pasi F, Orlandi A, Onorato LF, Gallino S (2011). A study of the 1 and 2 January 2010 sea-
 433 storm in the Ligurian Sea. *Advances in Science and Research*: 6, 109-115.
- 434 Parodi A, Boni G, Ferraris L, Siccardi F, Pagliara P, Trovatore E, Fofoula-Georgiou E,
 435 Kranzmueller D (2012). The “perfect storm”: From across the Atlantic to the hills of
 436 Genoa. *Eos Trans. AGU* 93(24),225.
- 437 Pérez-Alberti A, Trenhaile AS (2015). An initial evaluation of drone-based monitoring of
 438 boulder beaches in Galicia, northwestern Spain. *Earth Surface Processes and*
- 439 *Landforms*: 40(1), 105-111.
- 440 Rebora N, Molini L, Casella E, Comellas A, Fiori E, Pignone F, Siccardi F, Silvestro F,
 441 Tanelli S, Parodi A (2013). Extreme rainfall in the Mediterranean: what can we learn
 442 from observations? *Journal of Hydrometeorology*: 14, 906–922.
- 443 Rovere A, Casella E, Vacchi M, Parravicini V, Firpo M, Ferrari M, Morri C, Bianchi CN
 444 (2014). Coastal and marine geomorphology between Albenga and Savona (NW
 445 Mediterranean Sea, Italy). *Journal of Maps*: 1-9.
- 446 Scharstein D, Szeliski R (2002). A taxonomy and evaluation of dense two-frame stereo
 447 correspondence algorithms. *International Journal of Computer Vision*: 47, 7–42.
- 448 Seitz S, Curless B, Diebel J, Scharstein D, Szeliski R (2006). A comparison and evaluation
 449 of multi-view stereo reconstruction algorithms. *Proceedings of the CVPR '06 IEEE*
 450 *Computer Society Conference on Computer Vision and Pattern Recognition – Volume*
 451 *1. IEEE Computer Society: Washington, DC, pp. 519-526.*
- 452 Small C, Nicholls RJ (2003). A global analysis of human settlement in coastal zones.
 453 *Journal of Coastal Research*: 19, 584–599.
- 454 Szeliski R (2010). *Computer Vision: Algorithms and Applications*. Springer-Verlag: London.
- 455 Stockdon HF, Sallenger AH, List JH, Holman RA (2002). Estimation of shoreline position
 456 and change using airborne topographic lidar data. *Journal of Coastal Research*: 18,
 457 502–513.
- 458 Stumpf A, Malet JP, Kerte N, Niethammer U, Rothmund S (2013). Image-based mapping of
 459 surface fissures for the investigation of landslide dynamics. *Geomorphology*: 186, 12–
 460 27.
- 461 Taborda R, Silva A (2012). COSMOS: A lightweight coastal video monitoring system.
 462 *Computers & Geosciences*: 49, 248–255.
- 463 Ullman S (1979). The interpretation of structure from motion. *Proceedings of the Royal*
 464 *Society of London B*203: 405–426.

489 **FIGURE CAPTIONS**

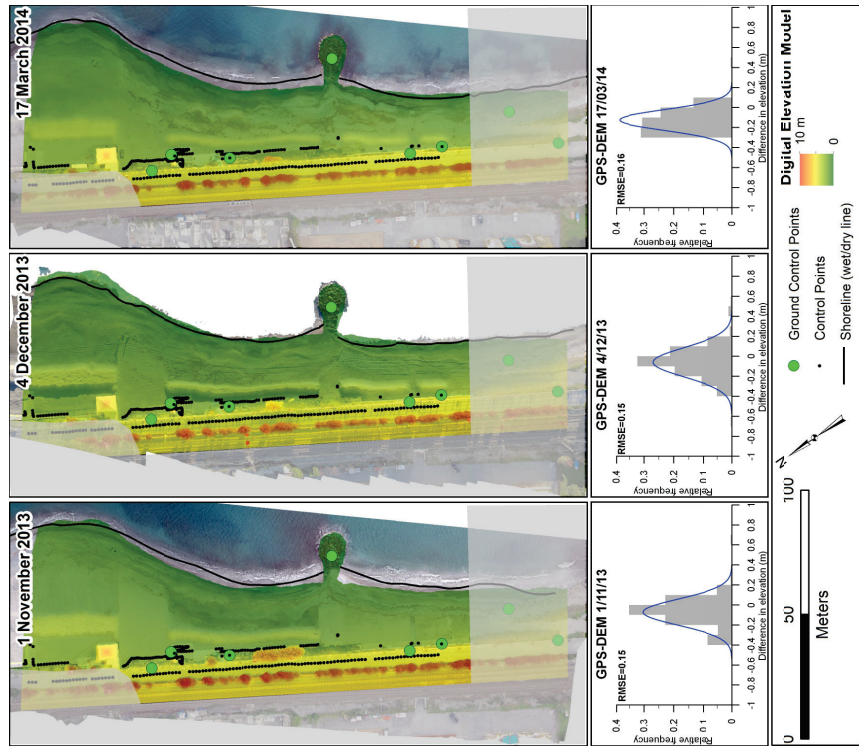


490
 491 **Fig.1 a) the shoreline and the nearshore area of Borghetto Santo Spirito showing the**
 492 **main geological and biological bottom coverages (Rovere et al., 2014). The figure**
 493 **also shows the shoreline traced as wet-dry line on orthophotos (1944-2003, data**
 494 **from Regione Liguria) and the shoreline surveyed with DGPS in June 2014 (data**
 495 **from Borghetto S.S. Municipality). The dashed blue arrow indicates the main**
 496 **sedimentary input from the Varatella River, while the solid blue arrow indicates the**
 497 **main littoral drift in the area (Rovere et al., 2014). The dashed red lines indicate the**
 498 **location of beach nourishment (labels indicate year and quantity of sediment used)**
 499 **and are indicative of the coastal stretch where the sediments have been damped**
 500 **onshore (data from Regione Liguria). Coastal defences and their year of**
 501 **construction are also indicated (data from Regione Liguria). b) Detail of a), area**
 502 **where the RPAS flights have been performed. The shoreline data have been**

465 Vacchi M, Rovere A, Schiaffino CF (2012). Monitoring the effectiveness of re-establishing
 466 beaches artificially: methodological and practical insights into the use of video
 467 transects and SCUBA-operated coring devices. *International Journal of the Society for*
 468 *Underwater Technology*: 30, 201–206.
 469 Verhoeven G (2011). Taking computer vision aloft – archaeological three-dimensional
 470 reconstructions from aerial photographs with PhotoScan. *Archaeological Prospection*: 18,
 471 67-73.
 472 Watts AC, Ambrosia VG, Hinkley EA (2012). Unmanned aircraft systems in remote sensing
 473 and scientific research: Classification and considerations of use. *Remote Sensing*: 4,
 474 1671-1692.
 475 Woodget AS, Carbonneau PE, Visser F, Maddock IP (2015). Quantifying submerged fluvial
 476 topography using hyperspatial resolution UAS imagery and structure from motion
 477 photogrammetry. *Earth Surface Processes and Landforms*: 40(1), 47-64.
 478

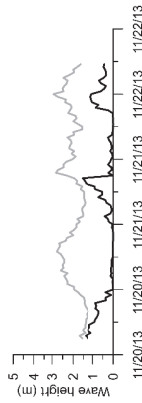
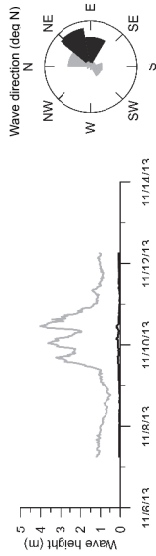
479
 480
 481
 482
 483
 484
 485
 486
 487
 488

503 provided by the Municipality of Borghetto S.S., and represent the wet-dry line at
 504 different years surveyed with DGPS. Bathymetric data have been provided by the
 505 Borghetto S.S. Municipality. c) Location of the study area in the Mediterranean Sea.

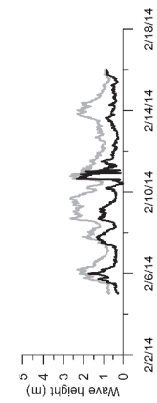
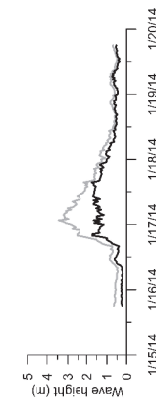
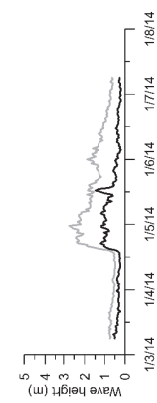
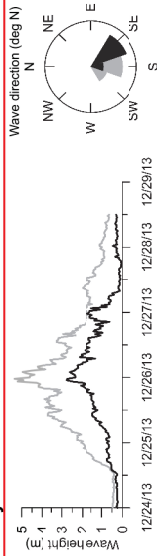


507 Fig.2 Orthophotos and Digital Elevation Models obtained from RPAS flights and SfM-
 508 MVS algorithms in the three surveys. The three boxes below the maps indicate the

Survey 1st November 2013

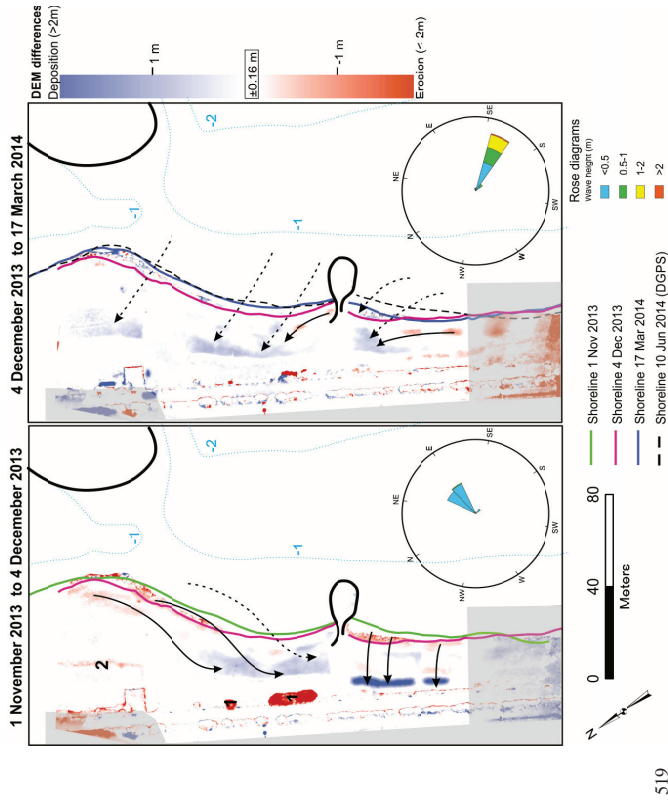


Survey 4th December 2013



Survey 17 March 2014

514 Fig.3 Wave height and direction for sea storms in the study area as recorded by the
 515 Buoy of Capo Mele (gray line and gray areas in the rose diagram) and wave height
 516 500 meters offshore in front of the study area calculated using MIKE21 spectral
 517 wave module (black line and black areas in the rose diagram). Dates are shown in
 518 MM/DD/YY format.



519

520 Fig.4 Difference between Digital Elevation Models obtained from our different

521 surveys (dates are indicated on top). Solid arrows indicate the movement of
 522 sediments that likely happened onshore, while dashed arrows indicate movement of
 523 sediments that likely involved sediment input from the submerged beach. Light gray
 524 areas indicate zones where there are few pictures overlapping (see Fig.2), therefore

525 where the DEM differences have been considered not reliable and are not discussed
526 in the text. The solid black lines indicate the structures for coastal defence, shown
527 also in Fig.1 and Fig.2. Bathymetric data have been surveyed in Summer 2013 by the
528 Borghetto S.S. Municipality and are the same in both frames. 1-Area where a grove
529 of reeds was cut in the time between the two surveys; 2-Area of 5-10 cm of erosion,
530 probably caused by strong NE winds that blew away sediment from the top of an
531 artificial dune (visible in Fig.2).